

# **Stereoscopic PIV adapted to gravity wave analysis**

by

Joachim Lengricht, Kai-Uwe Graw and Helmut Kronewetter<sup>1</sup>

Geotechnics and Hydraulic Engineering

Faculty of Economics, Civil Engineering Department

University of Leipzig

Marschnerstr. 31, D-04109 Leipzig, Germany

## **ABSTRACT**

Intrusive techniques of measuring the orbital velocities underneath gravity disturb the flow field in every case. Consequently, merely non-intrusive techniques can be applied to get information about the kinetics of the wave boundary layer, about the correlation between wind stresses and generated velocity profiles beneath the water surface, about the interaction of wave induced flow fields with oscillating water column energy converters and about wave energy transmission around permeable breakwaters.

A state-of-the-art stereoscopic particle image velocimeter was adapted to the wave flume of the University of Leipzig where the flow field is optically accessible from every point of view. The PIV set-up is based on the Scheimpflug principal recording images with the image sensor in the plane of best focus even when the object plane is not parallel to the lens principal plane. In this way, it is possible to rotate the image sensor into the plane of best focus without moving the camera objective itself. Keeping the camera view to the double-pulsed laser light sheet from an off-axis angle the Scheimpflug arrangement allows continuing the plane of best focus in the plane of the double-pulsed laser light sheet. Particularly for investigations underneath long-crested waves the Scheimpflug arrangement was found to be the best layout for stereoscopic PIV not only because of its ability to align the plane of best image but regarding to focal distances and camera angles. To reduce sub-pixel bias errors and to eliminate spurious vectors resulting from unmatched particle pairs, out-of-boundary motion, particle overlap, inter-particle correlations and optical imaging noise a non-post-interrogation method is used as correction technique which improves spatial resolution and vector yields.

Results obtained by the adapted stereoscopic PIV are presented for wave-structure interactions of monochromatic waves and a semi-submerged vertical wall, wave-structure interactions of regular waves propagating oblique towards a submerged horizontal plate and a breaking wave occurring due to the superposition of numerous wave components of a real sea state.

After the adaptation of the stereoscopic PIV-system to the specific conditions in a wave flume, it is now possible to map the flow conditions beneath gravity waves very sufficiently. It is possible to record wave-structure interactions very easily and rapidly by physical modelling. Time history velocity fields can be recorded and presented as three-dimensional velocity maps. The PIV system allows to investigate wave-induced motion in the vicinity of coastal structures in order to get information about turbulence parameters and wave energy dissipation as well as their distributions both locally and in time. Furthermore, complex wave motion can be investigated by observing and capturing the particular flow phenomena in a wave flume, e.g. real sea states consisting of numerous components superposing or decaying.

---

<sup>1</sup> TSI GmbH, Laser Diagnostics Division, Zieglerstr. 1, D-52078 Aachen



## 1. INTRODUCTION

Research about the interaction of wave induced flow fields with damping structures or wave energy converters was up to now mainly focused on the most exact description of the water surface displacement, i.e. the water surface profile  $\eta(t)$ , to describe the flow characteristics of the wave field without taking the flow patterns into account. While it is possible to calculate velocities and accelerations beneath undisturbed gravity waves even in the case of superposition of numerous wave components of a sea state, the interaction of wave induced flow fields with structures cannot be described analytically. Various flow patterns and diverse situations of disturbed orbital motion are created during wave-structure interaction. They depend on both the topical wave parameters and the shape of the structure, i.e. the laminar orbital motion underneath the undisturbed water surface turns to a turbulent motion when structures interact with the initial wave climate. The flow characteristics underneath gravity waves are closely related to dynamic actions of waves either to coastal structures or to the shore and possible sediment transport. These flow characteristics and induced turbulences have not been investigated systematically even quite a few approaches yields to remarkable results in specific cases.

Any intrusive technique of measuring the orbital velocities near the structure influences the orbital velocities themselves. Consequently, merely non-intrusive techniques can be applied to get information about the kinetics of the wave boundary layer, about the correlation between wind stresses and generated velocity profiles beneath the water surface, about the interaction of wave induced flow fields with oscillating water column energy converters and about wave energy transmission around permeable breakwaters.

Graw et al. (1990) demonstrated the difficulties related to the alterations of the velocity and the high resolution in time, which is needed to describe the instantaneous particle motion beneath gravity waves continuously. Lengright et al. (1994) and Lengright and Graw (1995) pointed out that whole field information about the velocities and accelerations underneath disturbed gravity waves can give important hints to analyse further aspects of wave propagation and turbulent interactions in the flow field. In contrast to point measurement techniques, the particle image velocimetry can guide to whole field information. This information is regarded when gravity waves interact with structures or the shore to detect not only the disturbed orbital velocity in its components but furthermore getting information about the local and temporal distribution of turbulent kinetic energy or vorticity around damping structures for instance.

Although particle image velocimetry was introduced to gravity wave analysis during the last years (e.g. by Gray et al. 1987, by Gray and Greated 1988 and by Greated et al. 1992) and latest performances were adjusted to coastal engineering laboratories (Gray and Bruce 1995) with the equipment presented here, it is possible to investigate regular and multi-chromatic wave motion with 3-D velocity measurements. Herewith a stereoscopic particle image velocimeter adapted to gravity wave analysis is presented and first results of the flow field analysis underneath gravity waves are given.

Therefore, a state-of-the-art stereoscopic particle image velocimeter was adapted to the wave flume of the University of Leipzig where the flow field is optically accessible from every point of view. The stereoscopic PIV for gravity wave analysis is designed similar to standard 2-D PIV systems with the supplement to measure the third velocity component, the z-component, which can be called the out-of-plane part of the velocity. This is done by a second camera and a camera configuration as described in chapter 2.

## 2. EXPERIMENTAL SET-UP

The individual parts of the PIV system beside the host computer are the integrated dual Nd:YAG Laser (25 mJ per Pulse, 20 Hz), the laserpulse light arm, the laser pulse synchronizer, the high resolution and the two high frame-rate cross correlation CCD camera (1K x1 K, 30 Hz frame rate) in our case equipped with high speed lenses (minimum

illumination 1:1,4 and focal length  $f=50\text{mm}$ ), the two high speed camera interfaces (transfer rate 100 MB/s), the multi channel digitizer and the image capture and analysis software (TSI Insight Stereo Ultra NT). This system allows a real-time image transfer to the host computer memory and a batch processing of up to 1,000 sequential images. The flow field is seeded with silver coated hollow particles (diameter  $13,8\ \mu\text{m}$ ) which scatter the incident laser light from the precisely definable illumination sheet pulsed at a rate of 20 Hz. The adapted stereoscopic PIV-system is shown in figure 1 schematically. Figure 2 gives an overview of the wave flume and the experimental arrangements at the University of Leipzig.

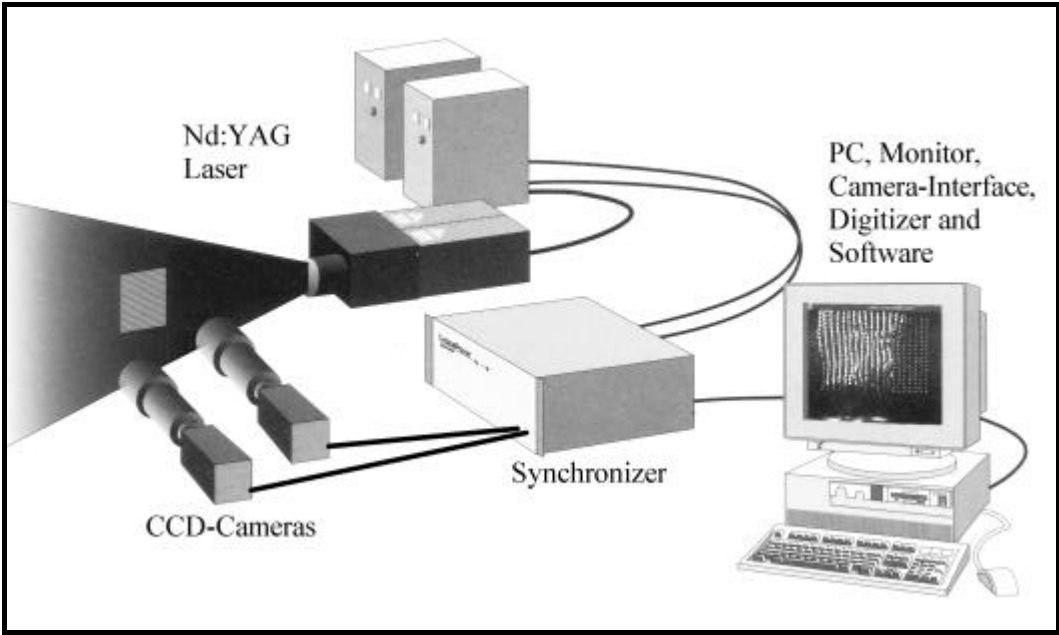


Fig. 1. Set-up of the stereoscopic PIV-system (schematically)



Fig. 2. Wave flume and experimental set-up at the university of Leipzig

As already mentioned for 3-D PIV measurements underneath gravity waves from two locations two cameras are viewing the flow field with two perspectives. When using a 2-D PIV equipment the x- and y-components of velocity are perpendicular to the optical axis of the one camera observing the flow field. In our case of measuring all three directions of the flow, the pairs of two-dimensional velocity vectors from each of the both cameras in one specific point are combined to get all the three velocity components in that particular point of the flow field. By combining these pairs of two-dimensional velocity vectors for every point in the area of interest a three-dimensional velocity field beneath gravity waves can be calculated for any instant of time of a wave-cycle.

The optical arrangements for stereoscopic particle image velocimetry are described in literature in detail (e.g. Raffel et al., 1998). The adapted PIV set-up is based on the Scheimpflug principal recording images with the image sensor in the plane of best focus even when the object plane is not parallel to the lens principal plane. In this way, it is possible to rotate the image sensor into the plane of best focus without moving the camera objective itself. The correct focus and tilt angles are attained when all of the particles within camera field of view are in good focus. Keeping the camera view to the double-pulsed laser light sheet from an off-axis angle the Scheimpflug arrangement allows continuing the plane of best focus in the plane of the double-pulsed laser light sheet. Because the image sensor is close to the lens optical axis, the image intensity is similar to the angular offset camera system (Bjorkquist, 1998). Particularly for investigations underneath long-crested waves the Scheimpflug arrangement was found out to be the best layout for stereoscopic PIV not only because of its ability to align the plane of best image but regarding to focal distances and camera angles. The adapted stereoscopic PIV-System with the Scheimpflug arrangement of the stereoscopic cameras is shown in figure 3 schematically.

Positioning the cameras in the Scheimpflug condition a perspective distortion is established to the images of both cameras observing the flow field, i.e. a rectangular area of interest in the light sheet fanned out by the Nd:YAG-laser is recorded as a trapezoid on the image sensors of both the right and the left camera. This is shown in principle in figure 4. When using the Scheimpflug arrangement the taken images have to be treated in a way that the velocity vectors represent no further the distorted image but the authentic area of interest in the laser-light-sheet. Therefore, a calibration procedure is necessary to measure and correct the perspective distortion due to the camera tilt and other image distortions in the optical system.

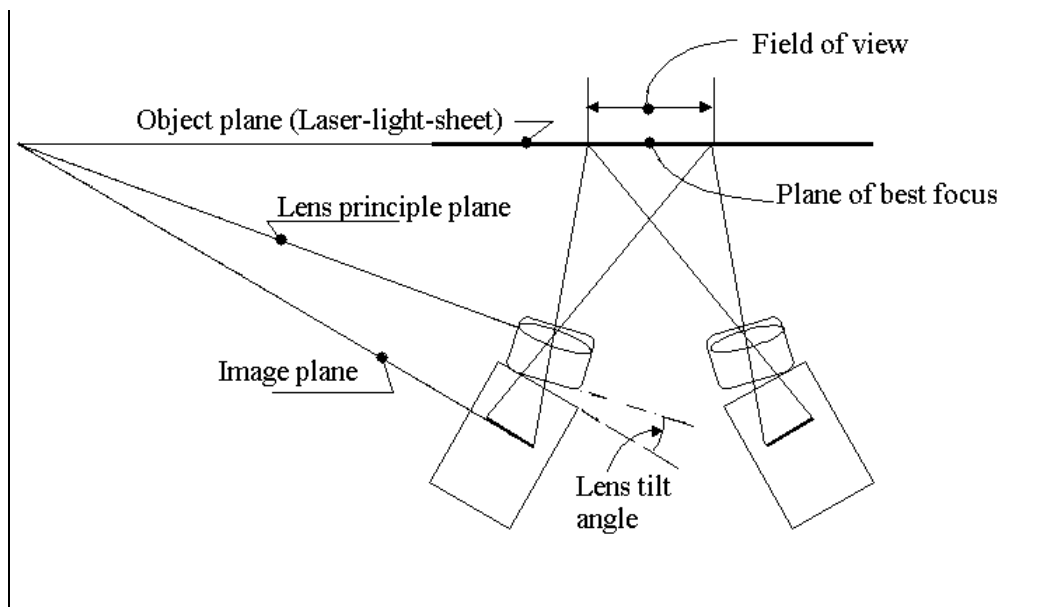


Fig. 3. Scheimpflug arrangement of the stereoscopic cameras (see Bjorkquist, 1998)

For calibrating the 3-D PIV-system, a rectangular grid of dots is aligned to the laser-light-sheet by a traverse facility. Calibration grid images are taken and analysed with up to fifth order calibration polynomial equations for each camera. By using these polynomials, high demands on the alignment of the cameras with sub-pixel precision can be neglected, because they allow to correct distortions caused by lens aberrations, distortions of the accessed area of interest as well as any other distortions in the optical system. At the end of the calibration routine, each point in the area of interest has a distinctive set of displacement factors. These displacement factors indicate the relation between the particle image displacement and the motion of a tracer particle in all three direction in the captured images.

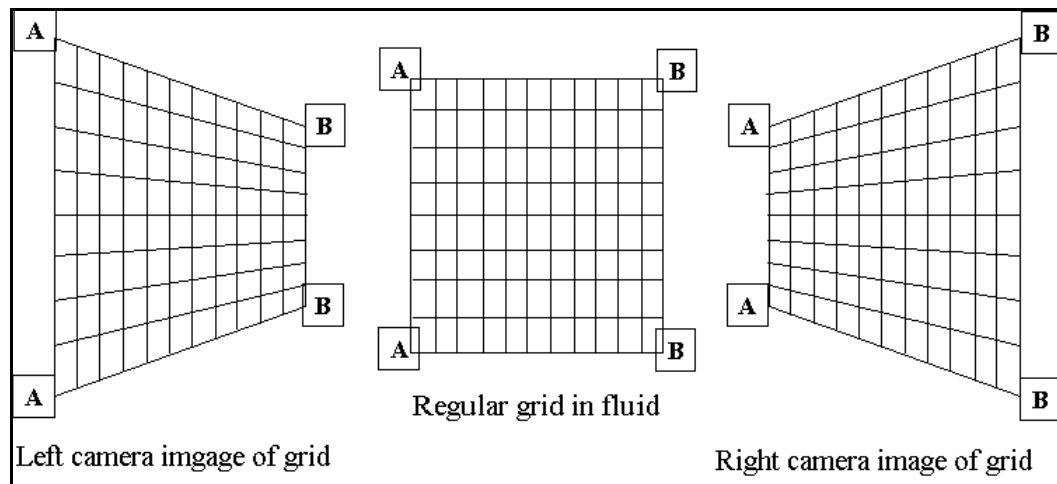


Fig. 4. Perspective effect due to camera tilt (see Bjorkquist, 1998)

To reduce sub-pixel bias errors and to eliminate spurious vectors resulting from unmatched particle pairs, out-of-boundary motion, particle overlap, inter-particle correlations and optical imaging noise a non-post-interrogation method is used as correction technique which improves spatial resolution and vector yields (Hart, 1998).

### 3. RESULTS AND DISCUSSION

Results obtained by the adapted stereoscopic PIV are presented for

- wave-structure interactions of monochromatic waves and a semi-submerged vertical wall,
- wave-structure interactions of regular waves propagating oblique towards a submerged horizontal plate and
- a breaking wave occurring due to the superposition of numerous wave components of a real sea state.

#### 3.1 Interaction of monochromatic waves and a semi-submerged vertical wall

The semi-submerged vertical wall is as well one important type of permeable breakwaters as a construction element of certain types of wave energy converters like the oscillating water column converter. The effect of this structure to the initial waves has been described by potential equations or energy balancing at the barrier. On the other

hand, it is known (Lengright et al. 1994) that the interaction of monochromatic gravity waves with the semi-immersed obstacle causes eddy motion in the wave induced flow field, which might influence the efficient operation of wave energy converters.

The flow patterns detected differ from each other depending on the actual parameters of the incoming waves, i.e. length, height and period. In general, the semi-submerged vertical wall disturbs the orbital paths beneath incoming waves. The water surface in front of the wall surpasses the peak amplitude of the undisturbed initial wave, which leads to a transformation of kinetic wave energy to potential energy. This leads to a difference in the potential, because the potential energy in the sheltered area is smaller than in front of the obstacle. The disarrangement of particle motion in front and around the obstacle depends intensely on the particular wave interacting with the obstacle. The exemplary results of the investigations are given for a wave out of the intermediate water depth range. The degree of obstruction by the semi-submerged vertical wall is 50% in that case..

Figure 5 reveals the interaction between the incoming monochromatic gravity wave and the semi-submerged thin vertical wall as an important design feature of coastal structures. The velocity vectors and the vorticity  $\mathbf{w}$  are shown for a discrete phase angle of the incoming wave represented by  $t/T=0.920$  as a discrete instant of time of the wave period. At this instant of time, the trough of the incoming wave has already reached the wall. A reverse energy difference is formed and a current against the propagation direction of the incoming wave is created. Moreover, this current generates eddy motion in front of the wall. Figure 5 depicts eddy formation in the flow field in terms of giving values for the vorticity in front of the obstacles. While the one eddy rotates clockwise (blue) the other vortex turns counter clockwise (red).

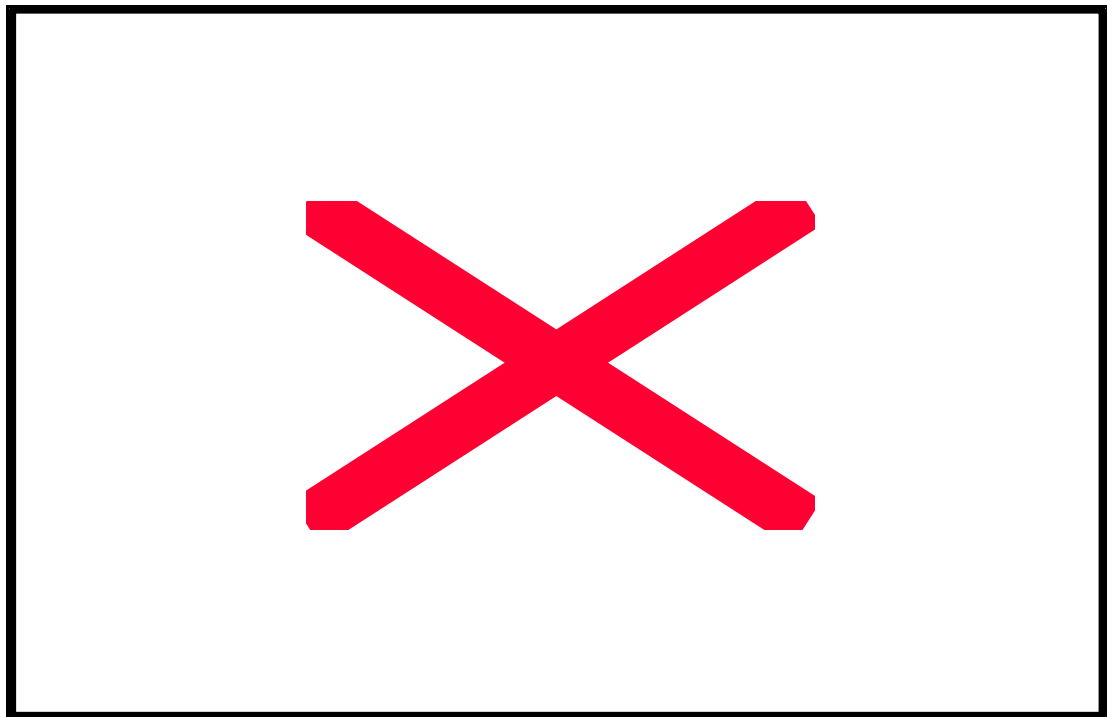


*Fig. 5. Velocity vectors and intensity of vorticity  $\mathbf{w}$  in the disturbed wave field at  $t/T=0.920$  (monochromatic intermediate water depth wave interacting with a semi-submerged vertical barrier)*

The velocity vectors and the vorticity  $\mathbf{w}$  are shown over a whole cycle of the incident wave at discrete instants of time in figure 6. In these frames, the velocity distributions around the semi-submerged barrier indicate the flow motion beneath the barrier during one cycle of oscillation of the initial wave. The sketches 6a to 6l illustrate the

oscillating motion around the semi-submerged vertical wall over a whole wave period at distinct phase angles of the incoming wave represented by  $t/T$  as discrete instants of time of the wave period.

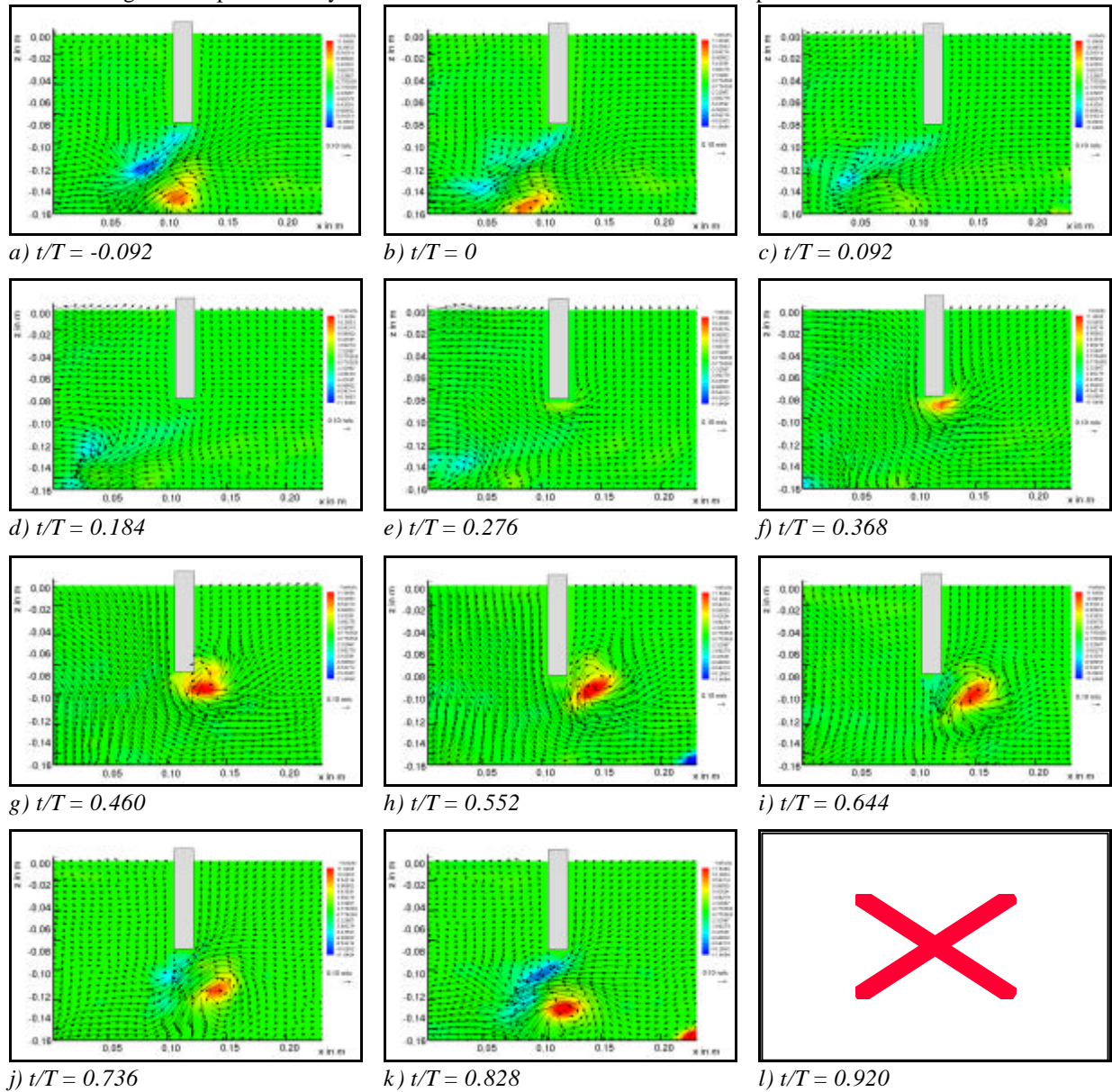


Fig. 6. Time history of the velocity field as vector plots and intensity of vorticity  $\omega$  in the disturbed wave field in constant time intervals  $\Delta t = 0.092$  s at discrete instants of time  $t/T$ , monochromatic intermediate water depth wave interacting with a semi-submerged vertical barrier

It can be observed that the irregular motion caused by the previous incoming wave is conserved until the water surface surpasses the peak amplitude of the undisturbed initial wave. In the sketches 6f and 6g, it can be noticed that an accelerated flux in the wave propagation direction is generated. This results from the potential difference as explained above because the amount of the potential energy is in the sheltered area is smaller than in front of the wave barrier. The in-flow flux induces eddy motion behind the breakwater as illustrated in sketches 6g to 6i by the rate of vorticity. When the trough of the initial wave reaches, the flow direction is changed due to the reverse

energy difference from the sheltered area to the front of the wall. Eddies formed behind the wall moves to the gap underneath the barrier against the wave propagation direction (see sketch 6j to 6l).

**3.2 Interaction of regular waves and a submerged plate**

Another feature of a permeable breakwater - the submerged horizontal plate - and its interaction with regular waves was investigated. The wave height reduction by the submerged plate as a wave filter is commonly known for several years. Using such a rigid horizontal plate to reduce the height of incoming waves has several advantages compared to solitary breakwaters. One of these advantages is to allow an ecologically desirable exchange of water between the open sea and the area to be protected. The discussion about the effects of a submerged horizontal plate was up to now reduced to the question whether an analysis of the damping effects only by a very accurate measurement of the first order water surface displacements is permissible or the shares of energy in higher order frequencies created as a result of the wave-structure interaction in the wake of the plate should be emphasised, e.g. by a Fourier's analysis. The flow patterns around the structure was not taken into account until now, i.e. the impact of this kind of breakwater to the velocity field induced around the plate and in the wake of the plate could not be clarified sufficiently yet.

Figure 7 shows the 2-D velocity fields recorded with the left and the right camera of the 3-D PIV-system (after a first pre-processing of the captured images) when a regular intermediate water wave interacts with a submerged horizontal plate. The wave propagation direction is from left to right. The waves reach the plate oblique to it, which might introduce a motion in the z-direction. Both cameras detect an eddy in the wake of the submerged horizontal plate due to both the transformation of wave energy above the plate and a flow around the plate, which is indicated by the direction of the velocity vectors underneath the plate.

In figure 8, the 3-D velocity field is calculated as mentioned in chapter 2 after a second pre-processing step. It can be seen that a slight part of "out of plane motion" is detected by stereoscopic particle image velocimetry. Thus, the velocity field and every other phenomena of wave-structure interaction can be recorded and analysed in not only one plane. This motion in z-direction was not taken into account when considering the interaction of this kind of permeable breakwater and the incident wave climate, i.e. a highly-developed non-intrusive measurement system was adapted to the physical examination of wave-structure interaction, even in case of a 3-D analysis.

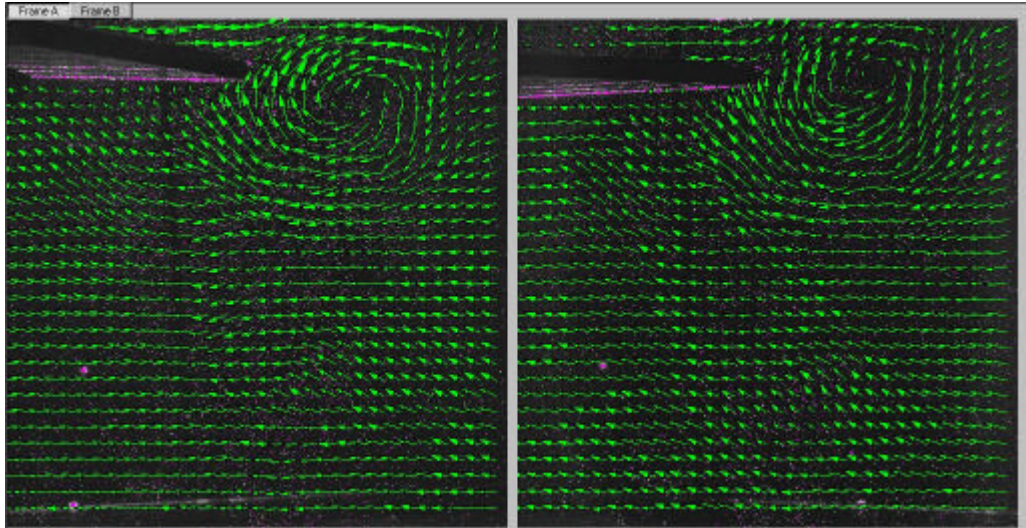


Fig. 7. Interaction of a regular intermediate water depth wave with a submerged horizontal plate.

2-D velocity fields after pre-processing the images recorded by the left and the right camera of the 3-D PIV-system.

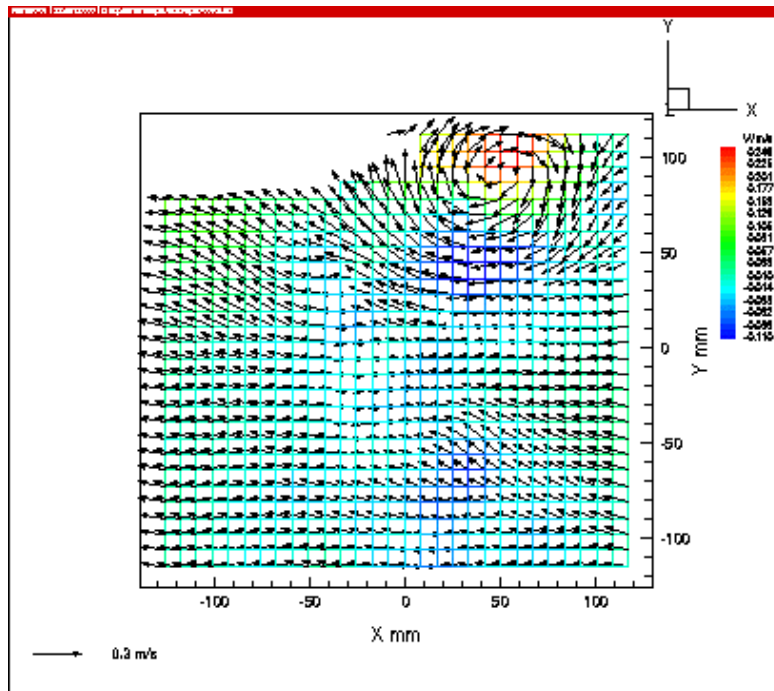


Fig. 8. 3-D Calculation of the velocity field: interaction of a regular intermediate water depth wave with a submerged horizontal plate as a primary breakwater

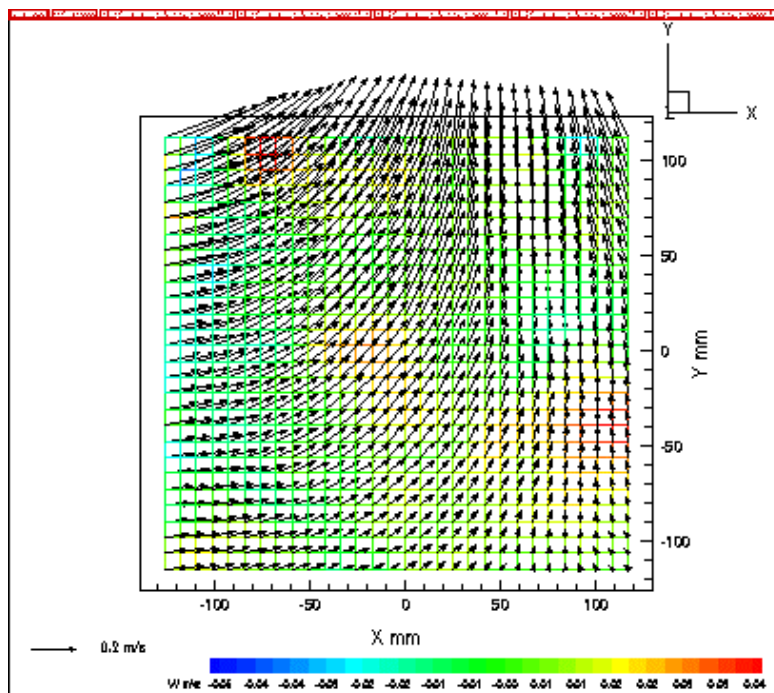


Fig. 9. Calculated 3-D velocity field as a three-dimensional vector plot underneath a broad-banded freak wave after two steps of pre-processing the images captured of both cameras

### 3.3 Breaking wave process of a transient wave

A further result of the 3-D PIV measurements underneath gravity waves is the three-dimensional velocity plot during the breaking process of a freak wave. Figure 9 reveals the three-dimensional velocity plot after two steps of pre-processing of the images captured by both of the cameras underneath a broad banded freak wave. It illustrates the particular condition in the flow field during the breaking process of that particular wave.

Freak waves are defined as transient waves, occur due to the superposition of numerous wave components of a real sea state, and are typically characterised by an extreme wave height. Up to now the exact description of the water surface profile  $h(t)$  of a freak wave in relative distances from the focus point was used to explain the flow characteristics. For the first time it is possible with the adapted stereoscopic PIV system to take the flow conditions underneath the free surface into account, i.e. to inspect the internal processes depending on different steepness of the wave front before the spilling process is caused. Figure 10 shows the calculated velocity field as a three-dimensional vector plot underneath a broad-banded freak wave after applying a post-processing routine to the pre-processed vector plots.

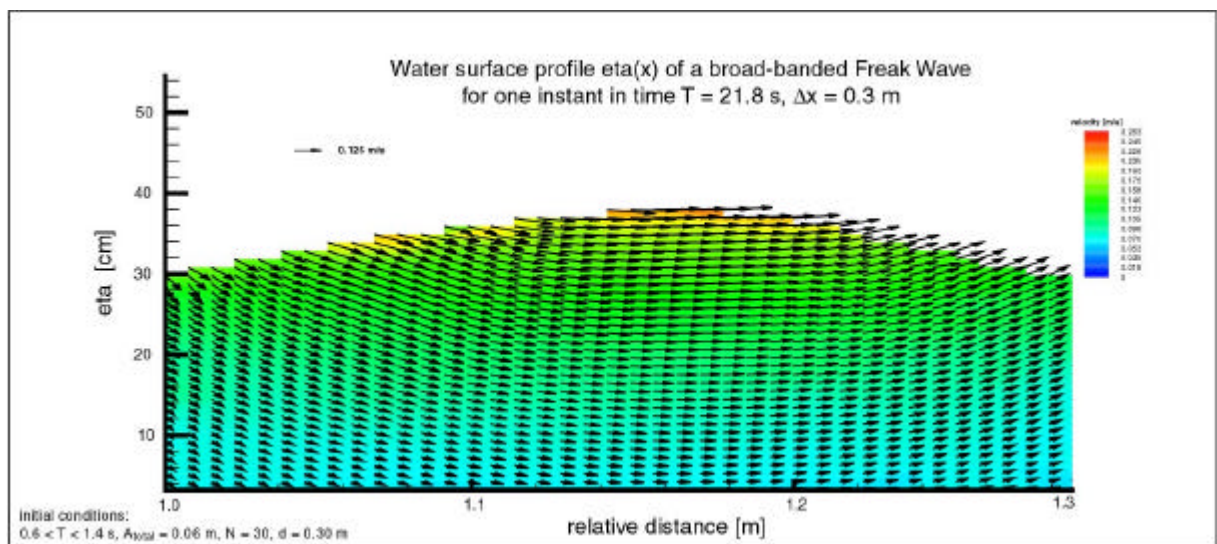


Fig. 10 Water surface elevation and velocity field as a three-dimensional vector plot underneath a broad-banded freak wave after post-processing

## 5. CONCLUSION

After the adaptation of the stereoscopic PIV-system (TSI Inc.) to the wave flume of the university of Leipzig, it is now possible to map the flow conditions beneath gravity waves very sufficiently. It is possible to record the wave-body interactions very easily and rapidly by physical modelling in the wave flume of the university of

Leipzig. Time history velocity fields can be recorded and presented in three-dimensional velocity maps. The PIV system allows to investigate wave-induced motion in the vicinity of coastal structures in order to get information about turbulence parameters and wave energy dissipation as well as their distributions both locally and in time. Furthermore, complex wave motion can be examined by observing and capturing the particular flow phenomena in a wave flume, e.g. real sea states consisting of numerous components superposing or decaying.

#### REFERENCES

Bjorkquist DC. 1998. Design and calibration of a stereoscopic PIV system. *Proc. 9<sup>th</sup> International Symposium on Applications of Laser Techniques to Fluid Mechanics*. Vol. 1, pp. 6.5.1-6.5.8, Lisbon, Portugal.

Graw K-U, Kaldenhoff H, Stieglmeier M. 1990. Optical measurement of orbital velocity. *Proc. 5<sup>th</sup> International Symposium on Applications of Laser Techniques to Fluid Mechanics*. Paper 8.1. Lisbon, Portugal.

Gray C, Greated CA, Easson WJ, Fancey NE. 1987. The application of PIV to measurements under waves. *Proc. 2<sup>nd</sup> International Conference Laser Anemometry - Advanced Applications*, pp.281-287. Strathclyde, UK.

Gray C, Greated CA. 1988. The application of PIV to the study of water waves. *Optics Laser Eng* 9

Gray C, Bruce T. 1995. The application of particle image velocimetry (PIV) to offshore engineering. *Proc 5<sup>th</sup> International Offshore and Polar Engineering Conference (ISOPE)*. Vol. III, pp. 701-708. The Hague, The Netherlands.

Greated CA, Skyner DJ; Bruce T. 1992. Particle image velocimetry in the coastal engineering laboratory. *Proc 23rd Coastal Eng Conf*: 212-225. Venice, Italy:

Hart DP. 1998. The elimination of correlation errors in PIV processing. *Proc. 9<sup>th</sup> International Symposium on Applications of Laser Techniques to Fluid Mechanics*. Vol. 1, pp. 13.3.1-13.3.8, Lisbon, Portugal.

Lengright J, Kaldenhoff H, Graw K-U. 1994. Measuring wave induced turbulence near structures. *Proc. International Symposium: Waves – Physical and Numerical Modelling*. Vol. I, pp. 80-89. Vancouver, Canada.

Lengright J, Graw K-U. 1995. Flow field analysis beneath gravity waves. *In: Flow Visualization and Image Processing of Multiphase Systems*. ASME, FED 209, pp. 57-64. New York, U.S.A.

Raffel M, Willert CE, Kompenhans J. 1998. Particle image velocimetry. *Springer*. Berlin/Heidelberg.